

Inhaled Dry Powder Formulation of Tamibarotene, a Broad-Spectrum Antiviral against Respiratory Viruses Including SARS-CoV-2 and Influenza Virus

Qiuying Liao, Shuofeng Yuan,* Jianli Cao, Kaiming Tang, Yingshan Qiu, Han Cong Seow, Rico Chi-Hang Man, Zitong Shao, Yaoqiang Huang, Ronghui Liang, Jasper Fuk-Woo Chan, Kwok-Yung Yuen, and Jenny Ka-Wing Lam*

In response to the epidemic and pandemic threats caused by emerging respiratory viral infections, a safe and efficient broad-spectrum antiviral therapy at early onset of infection can significantly improve patients' outcome. Inhaled dry powder is easy to administer and delivers antiviral agent directly to the primary site of infection, thereby minimizing systemic side effects. Here, spray freeze drying (SFD) technique is employed to formulate tamibarotene, a retinoid derivative with broad-spectrum antiviral activity, as inhalable powder. The SFD tamibarotene powder exhibits desirable physicochemical and aerodynamic properties for inhalation. Pulmonary delivery of tamibarotene powder results in rapid absorption and higher bioavailability compared with intraperitoneal injection of unformulated drug in animals. More importantly, inhalation or intranasal delivery of SFD tamibarotene formulation displays broad-spectrum antiviral activity against severe acute respiratory syndrome coronavirus 2 (SARS-CoV-2), Middle East respiratory syndrome coronavirus, and pandemic 2009 influenza A virus (H1N1) in mouse and hamster models by targeting lower or upper airways, and the efficacy is comparable or superior to the commercially available antivirals remdesivir and zanamivir against specific virus. These results present a promising strategy to combat various respiratory viral infections including SARS-CoV-2 and influenza virus, or even co-infection.

1. Introduction

Respiratory viral infections are posing significant threat to global public health. Influenza viruses have a long history of affecting human health, causing hundreds of thousand deaths per year, with possibility of future pandemics.^[1] In recent years, there is a number of outbreaks caused by previously unknown coronavirus leading to severe human respiratory diseases, including the severe acute respiratory syndrome (SARS) in 2003,^[2] the Middle East respiratory syndrome (MERS) in 2012,^[3] and the most recent Coronavirus Disease 2019 (COVID-19) caused by SARS coronavirus 2 (SARS-CoV-2), which is declared as a global pandemic in 2020.^[4] They are highly pathogenic and contagious with severe morbidity and mortality, resulting in significant socioeconomic disruptions worldwide. While COVID-19 vaccine has been rapidly developed^[5] and some positive outcomes were seen with currently available therapeutics such as dexamethasone^[6] and


Q. Liao, Dr. Y. Qiu, H. C. Seow, R. C.-H. Man, Z. Shao, Dr. J. K.-W. Lam
Department of Pharmacology and Pharmacy
LKS Faculty of Medicine
The University of Hong Kong
21 Sassoon Road, Pokfulam, Hong Kong SAR, China
E-mail: jkwlam@hku.hk

Dr. S. Yuan, J. Cao, K. Tang, Y. Huang, R. Liang, Dr. J. F.-W. Chan,
Prof. K.-Y. Yuen
State Key Laboratory of Emerging Infectious Diseases
Carol Yu Centre for Infection
Department of Microbiology
LKS Faculty of Medicine
The University of Hong Kong
Pokfulam, Hong Kong SAR, China
E-mail: yuansf@hku.hk

Dr. J. F.-W. Chan, Prof. K.-Y. Yuen
Department of Clinical Microbiology and Infection Control
The University of Hong Kong-Shenzhen Hospital
Shenzhen, Guangdong Province 518053, China

Dr. J. F.-W. Chan, Prof. K.-Y. Yuen
Hainan Medical University-The University of Hong Kong Joint Laboratory
of Tropical Infectious Diseases
Hainan Medical University
Haikou Hainan Province 571199, China

Dr. J. K.-W. Lam
Advanced Biomedical Instrumentation Centre
Hong Kong Science Park
Shatin, New Territories, Hong Kong SAR, China

 The ORCID identification number(s) for the author(s) of this article can be found under <https://doi.org/10.1002/adtp.202100059>

© 2021 The Authors. *Advanced Therapeutics* published by Wiley-VCH GmbH. This is an open access article under the terms of the Creative Commons Attribution-NonCommercial-NoDerivs License, which permits use and distribution in any medium, provided the original work is properly cited, the use is non-commercial and no modifications or adaptations are made.

DOI: 10.1002/adtp.202100059

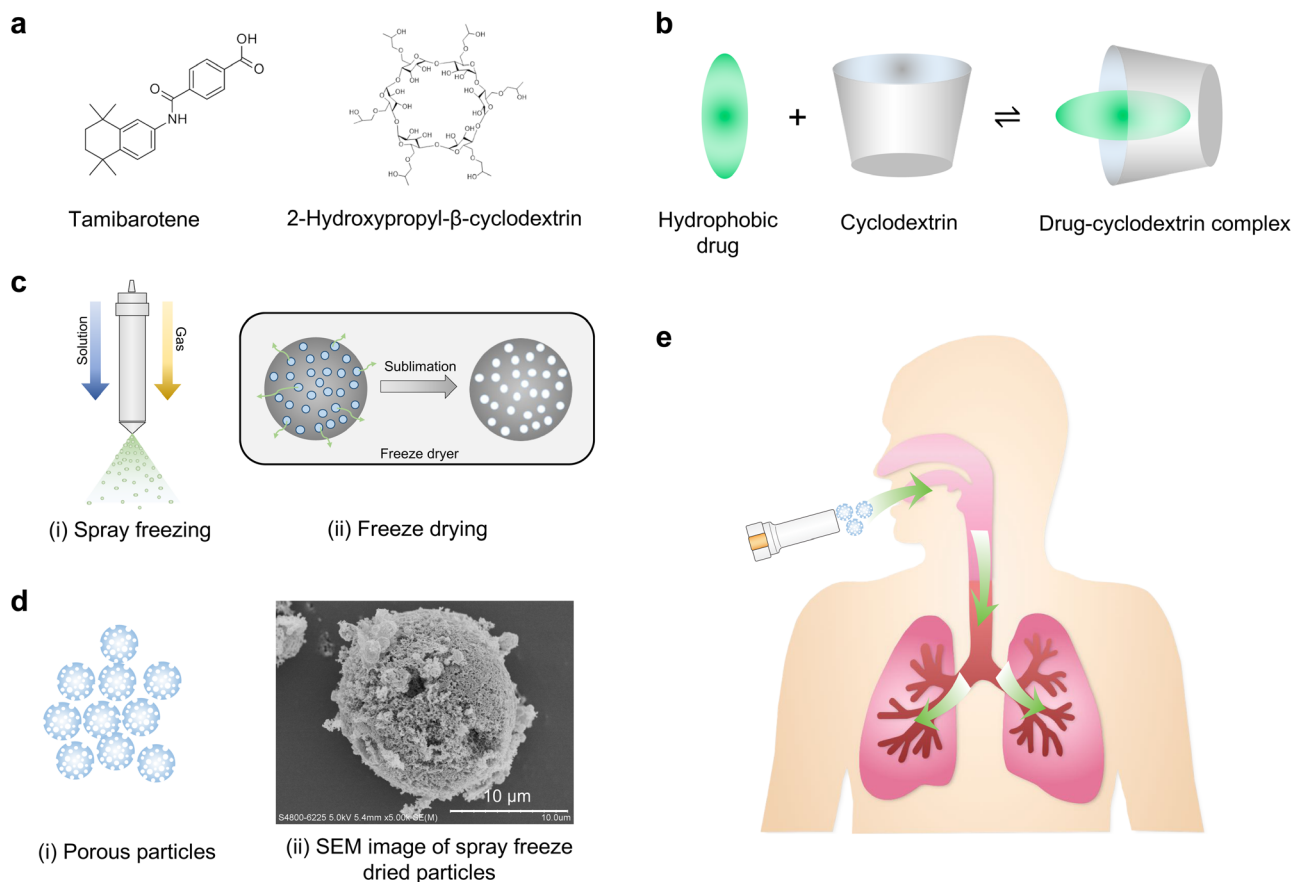


Figure 1. Formulation of tamibarotene into inhalable dry powder using spray freeze drying technique with cyclodextrin used as the sole excipient. a) Chemical structure of tamibarotene and 2-hydroxypropyl- β -cyclodextrin (HPBCD). b) Hydrophobic drug and cyclodextrin form inclusion complex by hydrophobic interaction. c) Two steps are involved in spray freeze drying: i) spray freezing, atomization of liquid by a nozzle into cryogen forming frozen particles; ii) freeze drying, sublimation of solvent and formation of dried porous particle. d) Spherical porous dry powder produced by spray freeze drying: i) schematic illustration; ii) scanning electron microscopy image under 5000 \times magnification. e) Oral inhalation of porous particles to deliver drug into the deep lung region.

neutralizing antibody cocktail,^[7] the interim results of the WHO Solidary Trial suggested that some of the current treatment regimens had very limited effect on hospitalized COVID-19 patients in terms of the overall mortality, ventilation requirement, and duration of hospital stay.^[8] Therefore, discovery of additional effective antivirals for COVID-19 is urgently needed. Moreover, epidemic and pandemic outbreak of influenza or coronavirus may occur unpredictably. Early administration of a broad-spectrum antiviral agent could be an effective strategy to control the spread of infections.

Lipid metabolic reprogramming in host cell was demonstrated to be a druggable target to interfere with viral multiplication.^[9] We recently demonstrated that retinoid derivative AM580 blocks host lipogenic transactivation by binding with the sterol regulatory element binding protein (SREBP).^[10] The suppressed SREBPs-mediated lipogenesis, thereby, affects the building of membrane blocks, energy supply, and post-translational protein modification that influence propagation of diverse groups of viruses.^[11] The importance of SREBP regulatory pathway has been implicated in the life cycle of hantavirus which is dependent on lipid synthesis for virus entry and membrane fusion

process.^[12] In our previous studies, reduced double-membrane vesicles formation and viral protein palmitoylation are two important consequences of AM580-mediated SREBP inhibition for coronavirus and influenza A virus, respectively,^[10,13] suggesting its potential as broad-spectrum antiviral agent. Tamibarotene (previously known as AM80) (**Figure 1a**), an analogue of AM580, is an orally active retinoid for the treatment of acute promyelocytic leukemia (currently marketed in Japan only). With an antiviral activity comparable to AM580, tamibarotene has an established safety profile in human with milder adverse effects than other retinoic acids.^[14] Tamibarotene is available as oral tablet, which is difficult to achieve robust antiviral activity in the respiratory tract due to inadequate lung distribution following oral administration. When high dose is administered to compensate the insufficient lung distribution, toxic side effects are expected because of the extensive systemic exposure. Pulmonary delivery of tamibarotene could increase local drug concentration in the lung and reduce unintended distribution, therefore maximizes the antiviral effect in the respiratory tract with a lower dose.

Pulmonary delivery of dry powder formulations has several advantages such as good stability and easy administration with

the possibility of high dose antimicrobial delivery which is crucial for the treatment of lung infections.^[15] It also avoids the risk of contamination and transmission of viral particles associated with the use of nebulizer.^[16] The major challenge of formulating tamibarotene for pulmonary delivery is its low water solubility. To address this issue, cyclodextrin (CD) or its derivatives (Figure 1a), which are known to improve drug solubility through complexation (Figure 1b), are incorporated in the formulation. CDs belong to a class of cyclic oligosaccharides with a hydrophobic internal cavity and hydrophilic external surface, which can form inclusion complexes with drug molecules through hydrophobic interaction, thereby enhancing drug solubility.^[17] Spray freeze drying (SFD) is the method of choice to prepare inhaled powder formulation of tamibarotene because it typically produces porous particles with low density, which can improve the rate of drug dissolution and aerosol performance.^[18] SFD is a two-stage particle engineering technique (Figure 1c), in which the feed solution is sprayed into a cryogen such as liquid nitrogen where the atomized particles are instantaneously frozen, followed by the sublimation of solvent at low pressure and temperature, leading to the formation of dried porous particles (Figure 1d). The particle size, morphology, and the aerosol properties of SFD particles can be controlled by manipulating the operation parameters such as atomizing gas flow rate and drying temperature.^[19]

The current study aimed to develop SFD powder formulation of tamibarotene that can be used as an inhalable broad-spectrum antiviral therapy against various respiratory viral infections (Figure 1e). Using 2-hydroxypropyl- β -cyclodextrin (HPBCD) as the sole excipient to improve drug solubility, the physicochemical properties, aerosol performance, and pharmacokinetic profile of the SFD formulation were investigated. Moreover, the antiviral efficacy of the powder formulations against coronaviruses (SARS-CoV-2 and MERS-CoV) and influenza A were studied in animal models following pulmonary delivery and intranasal delivery.

2. Results

2.1. Physicochemical and Aerosol Properties of SFD Tamibarotene Powder

Three dry powder formulations of tamibarotene were initially prepared with different drying conditions (Table S1, Supporting Information). A2-TFN formulation, which contained HPBCD and tamibarotene at 2:1 molar ratio prepared by SFD using a two-fluid nozzle for atomization, was identified for further investigation in this study due to its favorable aerosol properties for inhalation. The production yield of A2-TFN was 66.3% and the measured drug loading was closed to the theoretical value of 10.2% w/w. The morphology of tamibarotene powder before and after SFD was visualized by scanning electron microscopy (SEM) (Figure 2a). Compared to the unformulated tamibarotene which displayed rod-shape crystalline structure with varied length, A2-TFN powder exhibited porous and spherical structures. Particles of A2-TFN formulation were small in size (<10 μm) and the particles appeared to be slightly aggregated. The volumetric particle size distribution measured with laser diffractometer was consistent with SEM images, with a median diameter of 5.75 ± 0.11

μm (Table S1, Supporting Information). For inhaled formulation, aerodynamic diameter is critical in determining the site of lung deposition following powder dispersion. Aerodynamic diameter between 1 and 5 μm is considered to be optimal for lung deposition.^[20] Therefore, we further measured the aerodynamic diameter of A2-TFN formulation by Next Generation Impactor (NGI) coupled with a Breezhaler operated at 90 L min^{-1} (Figure 2b). The mass median aerodynamic diameter (MMAD) was calculated as $1.86 \pm 0.44 \mu\text{m}$, which is within the particle size range for effective lung deposition. The emitted fraction (EF) and fine particle fraction (FPF) were around 95% and 65%, respectively, demonstrating that A2-TFN powder could exit the inhaler and aerosolize efficiently with excellent lung deposition. Notably, the MMAD of the SFD powder was smaller than its volumetric size. This could be attributed to the low density of porous particles which facilitate powder aerosolization and reduce interparticle attraction. Moreover, particles with small aerodynamic diameter but large geometric size have the additional advantage of efficient lung deposition yet prolonged retention in the airway by avoiding rapid clearance.^[21] It is highlighted that the aerosol performance of the powder is also affected by the choice of inhaler device for powder dispersion.^[19b,22] Our data show that Breezhaler is a compatible inhaler device to our powder formulation for efficient aerosolization. Overall, the results from physicochemical and aerosol characterization suggested that A2-TFN formulation allows efficient powder deposition at the lower airways which coincides with the primary site of respiratory infection.

A good aqueous solubility is critical to ensure drug can be absorbed at concentration required for robust antiviral effect. As tamibarotene has a poor solubility, it is crucial to improve its solubility and dissolution rate. Dissolution study was performed with the fine particle dose (FPD) (which reflected the dose deposited in the lower airways) of the A2-TFN formulation. A burst-release profile was observed with a faster dissolution rate than the unformulated tamibarotene (Figure 2c). In A2-TFN formulation, $\approx 50\%$ of tamibarotene was released in the medium within the first 5 min and the cumulative drug concentration remained steady in the next 4 h. At the end of experiment (24 h), $\approx 60\%$ of drug was dissolved. It is speculated that there was recrystallization of tamibarotene due to supersaturation when tamibarotene was released from drug-CD complex at the initial phase of the dissolution.^[23] In contrast, the unformulated tamibarotene dissolved in a slow and steady pace, with $\approx 20\%$ of drug dissolved within the first hour. After 24 h, the cumulative dissolved drug from unformulated tamibarotene was significantly lower than that from A2-TFN powder (Student's *t*-test, $p < 0.01$), suggesting HPBCD inclusion complex also improved the solubility of tamibarotene in the dissolution medium. The inclusion complexation between HPBCD and tamibarotene was reflected by the Fourier-transform infrared (FT-IR) spectrum (Figure 2d). Characteristic peaks of tamibarotene (823, 1630, 1695, and 3038 cm^{-1}) were observed in the spectrum of unformulated tamibarotene and physical mixture, but absent in the spectrum of A2-TFN, indicating the successful formation of inclusion complex between the two components, thereby facilitating the formation of hydrogen bond with water. In the differential scanning calorimetry (DSC) thermogram (Figure 2e), the endothermic peak at $231 \text{ }^\circ\text{C}$ corresponding to the melting point of tamibarotene were

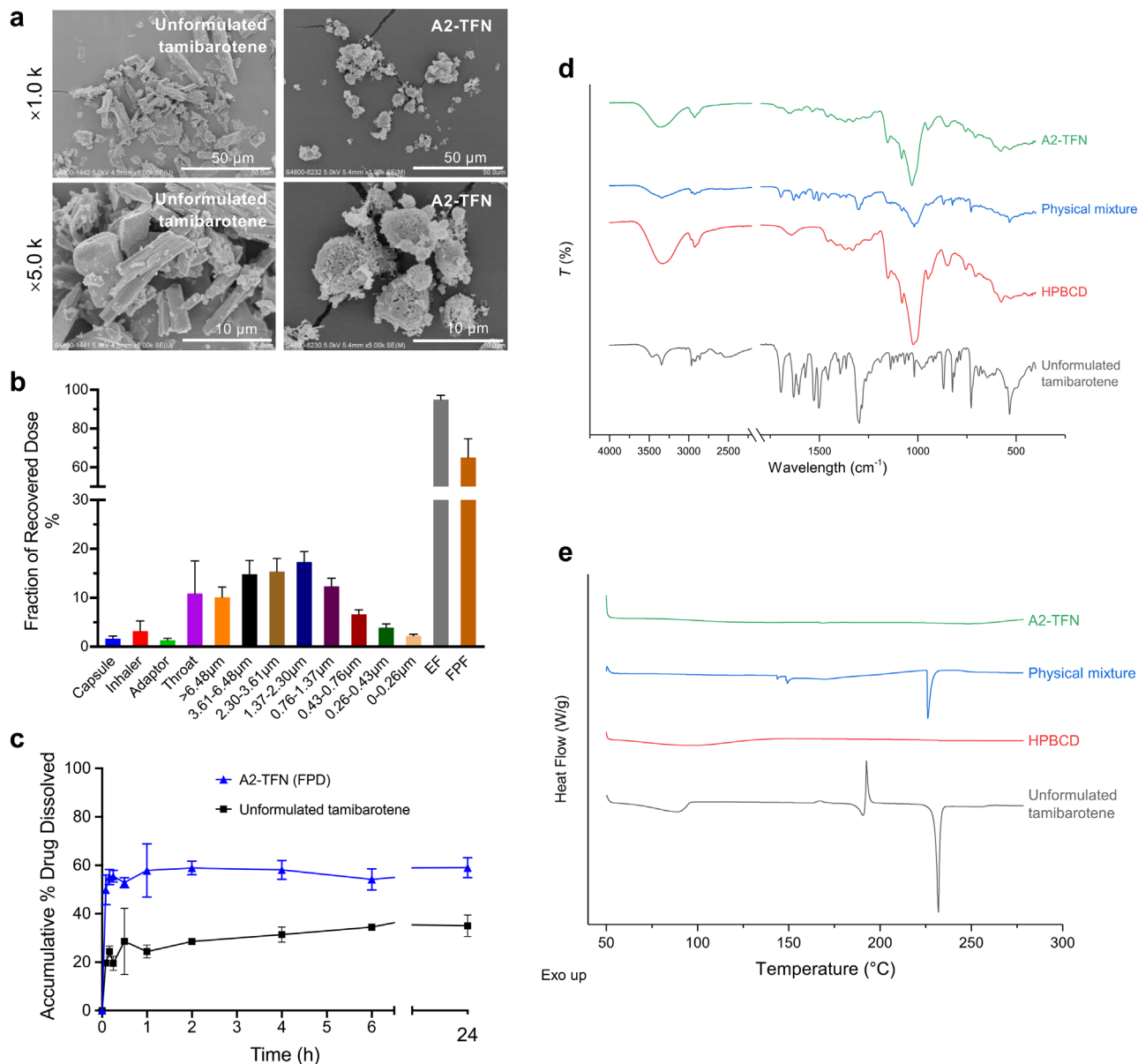


Figure 2. Physicochemical and aerosol properties of spray freeze dried tamibarotene powder (A2-TFN). a) Scanning electron microscope (SEM) images of unformulated tamibarotene and A2-TFN at 1.0k and 5.0k magnifications. Scale bar: 10 or 50 μm. b) Aerosol performance of A2-TFN powders evaluated by Next Generation Impactor (NGI) operated at 90 L min⁻¹, with the use of Breezhaler for powder dispersion. EF: emitted fraction (fraction of particle that exited the inhaler); FPF: fine particle fraction (fraction of particle with aerodynamic diameter below 5 μm); c) dissolution profile of fine particle dose (FPD—mass of particles with aerodynamic diameter below 5 μm) of A2-TFN compared with unformulated tamibarotene. Simulated lung fluid was used as dissolution medium. Data were presented as mean ± standard deviation (n = 3). d) Fourier-transform infrared spectroscopy (FT-IR) spectra and e) differential scanning calorimetry (DSC) thermograms of unformulated tamibarotene, HPBCD, physical mixture of HPBCD and tamibarotene, and A2-TFN powder. Negative peak in DSC thermogram represents endothermic event.

observed in unformulated tamibarotene and physical mixture, suggesting tamibarotene was in crystalline form before SFD. HPBCD and A2-TFN powder were amorphous as no significant thermal event was recorded. The transformation of tamibarotene from crystalline form to amorphous form after SFD also contributes to a faster dissolution rate.^[24] Consequently, the enhanced dissolution rate can lead to fast drug absorption before the undissolved powders are removed from the airways by the phagocytosis clearance action.

2.2. In Vivo Pharmacokinetic Profile

The pharmacokinetic profile of A2-TFN powder formulation delivered by intratracheal (i.t.) insufflation was compared with unformulated tamibarotene suspension administered by intraperitoneal (i.p.) injection in healthy BALB/c mice (**Figure 3**). The pharmacokinetic parameters of i.t. and i.p. groups are shown in **Table 1**. For the i.t. group, tamibarotene concentration reached the maximum level in 5 min ($T_{max} = 5$ min) in both plasma and

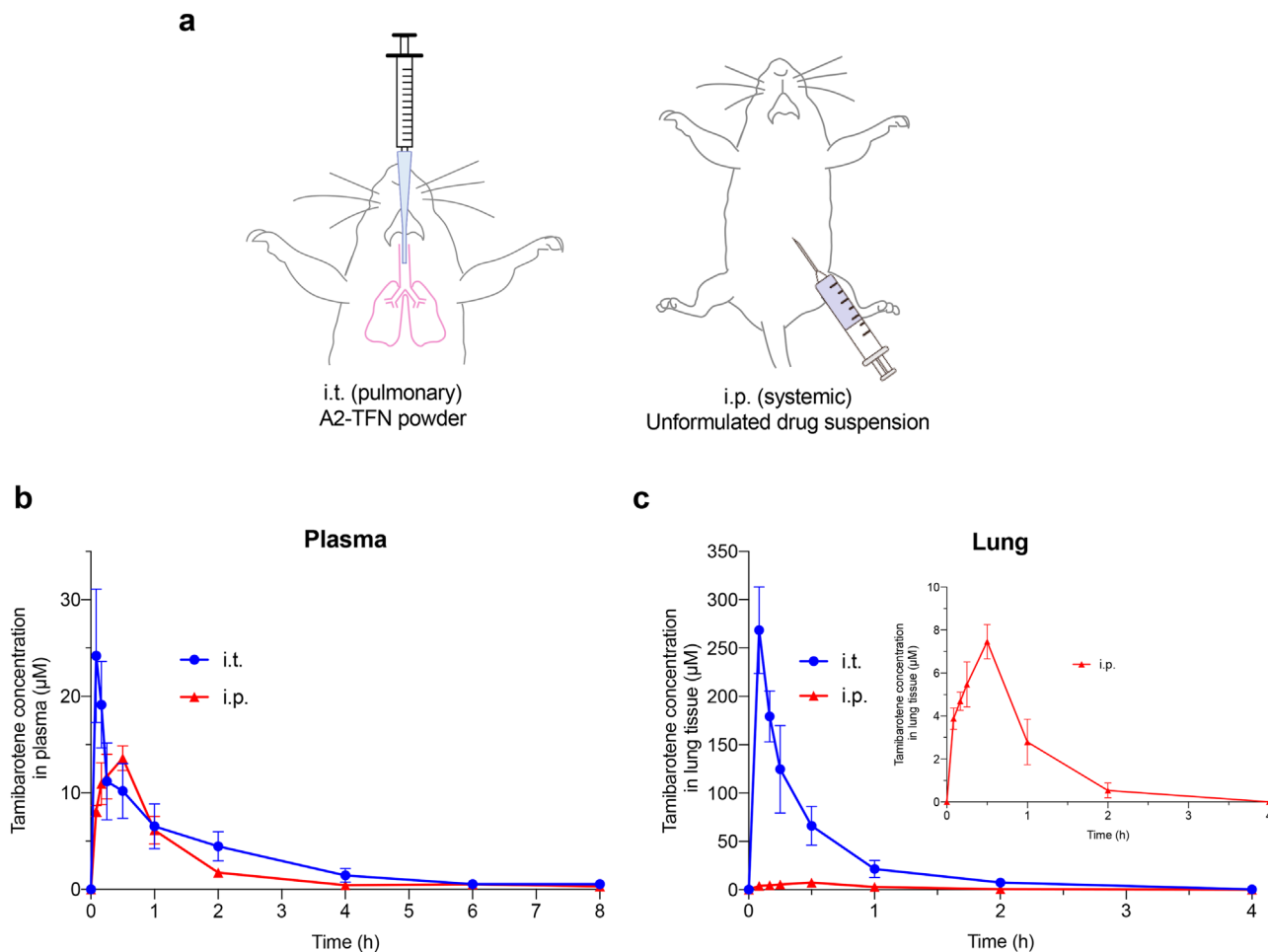


Figure 3. Pharmacokinetic profile of tamibarotene. a) Tamibarotene was administered to healthy BALB/c mice either as A2-TFN powder formulation via the intratracheal (i.t.) route or as unformulated suspension (in 0.1% DMSO) via the intraperitoneal (i.p.) route. A dose of 5 mg kg^{-1} tamibarotene was administered. b) Tamibarotene concentration–time curve in plasma. c) Tamibarotene concentration–time curve in the lung tissues. Data were presented as mean \pm standard deviation ($n = 5$).

Table 1. Pharmacokinetic parameters of tamibarotene following intratracheal (i.t.) administration of A2-TFN powder formulation and intraperitoneal (i.p.) injection of drug suspension to BALB/c mice. Parameters presented include maximum concentration (C_{max}), time to reach C_{max} (T_{max}), half-life ($T_{1/2}$), area under the curve (AUC), and mean residence time (MRT). These parameters were obtained by non-compartment analysis. For calculation purpose, drug concentration at 4 h post i.p. administration and beyond was treated as zero for non-compartmental analysis (NCA) modeling with manual fitting. EC_{50} of tamibarotene against MERS-CoV were obtained from our previous study.^[10] Data were presented as mean \pm standard deviation ($n = 5$).

Route and dosage form	Tissue	C_{max}	T_{max} [min]	$T_{1/2}$ [h]	$\text{AUC}_{0-8 \text{ h}}$ [$\mu\text{g}\cdot\text{h mL}^{-1}$]	$\text{AUC}_{0-\infty \text{ D}}$ [$\mu\text{g}\cdot\text{h mL}^{-1}$]	$\text{MRT}_{0-8 \text{ h}}$ [h]	EC_{50} [μM]		
								SARS-CoV-2	MERS-CoV	H1N1
i.t. (pulmonary) A2-TFN powder	Plasma	$25.1 \pm 4.8 \mu\text{M}$ ($8.8 \pm 1.7 \mu\text{g mL}^{-1}$)	5	1.7 ± 0.2	$8.5 \pm 1.0^*$	1.8 ± 0.2	1.8 ± 0.2			
	Lung	$268.4 \pm 44.7 \mu\text{M}$ ($94.2 \pm 15.7 \mu\text{g mL}^{-1}$)	5	0.5 ± 0.1	$36.0 \pm 4.8^{\#}$	7.2 ± 1.0	0.5 ± 0.1	5.8 ± 1.2	0.32 ± 0.026	1.68 ± 0.98
i.p. (systemic) Drug suspension	Plasma	$14.2 \pm 0.9 \mu\text{M}$ ($5.0 \pm 0.3 \mu\text{g mL}^{-1}$)	30	1.8 ± 0.4	$6.0 \pm 0.5^*$	1.5 ± 0.2	1.5 ± 0.2			
	Lung	$7.4 \pm 0.9 \mu\text{M}$ ($2.6 \pm 0.3 \mu\text{g mL}^{-1}$)	30	0.5 ± 0.08	$2.4 \pm 0.3^{\#}$	0.5 ± 0.06	0.6 ± 0.2			

* $p < 0.01$, # $p < 0.001$, when comparing same tissue between two groups, Student's t -test.

lung tissues. This observation was in line with the rapid dissolution of A2-TFN powder and hence fast absorption of drug following lung deposition. The drug concentration in plasma and lung tissues declined with an elimination half-life of 1.7 and 0.5 h, respectively. While tamibarotene in plasma maintained above the detectable level up to 8 h, it became undetectable in lung tissues after 4 h post-administration. For the i.p. group, an absorption phase is seen in the first 30 min after administration. The T_{max} for both plasma and lung tissues was 30 min. C_{max} in plasma following i.p. injection ($5.0 \pm 0.3 \mu\text{g mL}^{-1}$, equivalent to $\approx 14 \mu\text{M}$) was lower than that of i.t. administration ($8.8 \pm 1.7 \mu\text{g mL}^{-1}$, equivalent to $\approx 25 \mu\text{M}$). This was probably due to the slower rate of drug absorption after i.p. injection than i.t. insufflation. The C_{max} in the lung tissues following i.t. administration was 36-fold higher than that following i.p. administration ($p < 0.001$, Student's *t*-test). Most importantly, after i.t. administration, the C_{max} of tamibarotene in the lung is 46-fold higher (for SARS-CoV-2), 838-fold higher (for MERS-CoV), and 159-fold higher (for H1N1) than its antiviral EC_{50} , respectively (Table 1), which ensures a favorably high local concentration in the lung for efficient suppression of virus replication. As expected, the AUC_{0-8h} in the lung tissue following i.t. administration was significantly higher (15-fold) than that of i.p. injection ($p < 0.001$, Student's *t*-test). The AUC_{0-8h} in plasma following i.t. administration was also significantly higher than that of i.p. injection ($p < 0.01$, Student's *t*-test). The pharmacokinetic study showed that pulmonary delivery of A2-TFN formulation exhibited a rapid drug absorption which was superior to the i.p. administration of unformulated drug suspension. More importantly, higher bioavailability was achieved by pulmonary delivery of A2-TFN dry powder while systemic administration of tamibarotene displayed poor lung distribution. Our result demonstrated that pulmonary delivery of A2-TFN powder could be a promising approach to deliver tamibarotene for local antiviral action in the respiratory tract.

2.3. In Vivo Antiviral Efficacy

With the aim to develop an inhalation therapy of a safe and potent broad-spectrum antiviral in response to the emerging and re-emerging epidemic and pandemic threats caused by respiratory viral infections, we further investigated the in vivo prophylactic protection against coronaviruses and influenza A virus in animal models following i.t. administration of A2-TFN powder.

2.3.1. Against SARS-CoV-2

First, we investigated the in vivo antiviral effect of A2-TFN powder against SARS-CoV-2 using a recently established disease model in golden Syrian hamster^[25] (Figure 4). Single dose of A2-TFN powder or remdesivir solution was delivered via i.t. administration to the first two groups of hamsters, while the third group was treated with i.t. administration of phosphate buffer saline (PBS) as vehicle control. The dose of tamibarotene and remdesivir was 5 mg kg^{-1} . At 2 h post-administration, when the residual tamibarotene concentration in the lung is estimated to be above the EC_{50} according to pharmacokinetic study, all the hamsters were intranasally (i.n.) challenged with 10^5 plaque-forming

units (p.f.u.) SARS-CoV-2 (Figure 4a). Expectedly, the vehicle-treated control hamsters developed the clinical signs of lethargy, hunched back posture, and rapid breathing starting from 2 days post-infection (d.p.i.), whereas the hamsters treated with A2-TFN or remdesivir did not develop clinical symptoms. The highest viral load and the most prominent histopathological change were expected on day 4 post-infection in this model. The lung tissues of hamsters were harvested to examine whether A2-TFN powder and remdesivir can protect the animal from SARS-CoV-2 infection. The viral RNA load and viral titer in the lung tissues of hamster receiving i.t. administration of A2-TFN and remdesivir was significantly lower than that of PBS-treated hamster ($p < 0.05$, one-way ANOVA with post-hoc multiple comparison) (Figure 4b,c). There was no striking difference in terms of both the viral load and viral titer in the hamster lung tissue between A2-TFN powder and remdesivir treatment ($p > 0.05$, one-way ANOVA). Histopathological study of the lung tissues at 4 d.p.i. was carried out to examine the disease severity (Figure 4d). Consistent with previous reports,^[25,26] diffuse lung damage, alveolar collapse, and massive inflammatory cell infiltration and exudation were seen in the lung tissue of hamsters treated with PBS. By contrast, the lung tissues of hamster treated with A2-TFN powder and remdesivir showed ameliorated histopathological morphology with a mild degree of bronchiolar and alveolar cell infiltration. Immunofluorescence staining results suggested that although SARS-CoV-2 nucleocapsid protein (NP) expression was seen in focal bronchiolar epithelial cells of both A2-TFN powder- and remdesivir-treated hamsters, the expression of NP in alveolar region were considerably reduced in these two groups when compared with PBS control group, indicating a restriction of SARS-CoV-2 spread upon drug treatment (Figure 4e). Collectively, these results indicated that pulmonary delivery of A2-TFN powder in hamster could provide antiviral protection against SARS-CoV-2 and improve viral infection-associated symptoms, with a protective effect comparable to that of remdesivir, an FDA-approved antiviral for the treatment of COVID-19.

We further investigated the pan-coronavirus antiviral potential of inhaled tamibarotene powder in human dipeptidyl peptidase 4 (hDPP4) transgenic C57BL/6 mice model. The results showed that a single dose of A2-TFN powder given by i.t. insufflation prior to virus challenge could also confer some protection to the mice from MERS-CoV infection, as evident by the significantly decreased viral load in the lung (Figure S2, Supporting Information).

2.3.2. Against Influenza A H1N1 virus

Next, we evaluated the prophylactic anti-influenza activity of tamibarotene formulation in BALB/c model (Figure 5). Prior to virus inoculation, a single dose of A2-TFN powder, unformulated tamibarotene suspension, zanamivir solution, or PBS was delivered to the lung of mice via i.t. administration. The dose of tamibarotene and zanamivir was 5 mg kg^{-1} . At 2 h post-administration, the animals were inoculated i.n. with 100 p.f.u. H1N1 virus and monitored for 14 days (Figure 5a). At 14 d.p.i., the survival rates of A2-TFN group and zanamivir group were 80% and 60%, respectively, while all the mice in PBS group and unformulated tamibarotene group reached humane

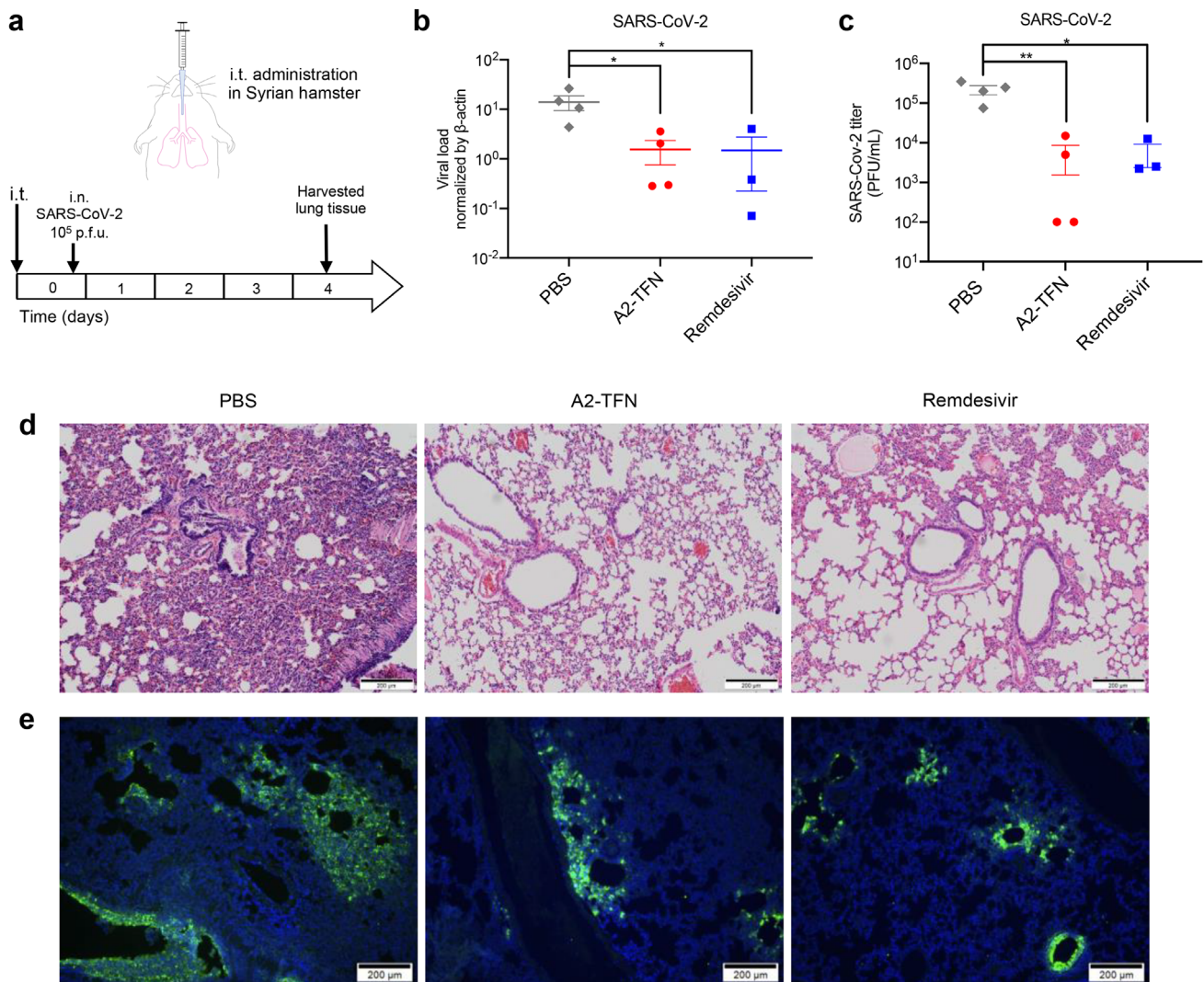


Figure 4. In vivo antiviral activity of tamibarotene formulation against SARS-CoV-2 for prophylactic protection. a) Schematic of i.t. administration in Syrian hamster and the schedule of experimental protocol. Each hamster received either PBS solution, A2-TFN powder, or remdesivir solution via intratracheal (i.t.) administration prior to intranasal (i.n.) inoculation of SARS-CoV-2. b) Lung tissue of infected hamsters were harvested at 4 days post-infection for viral load assay ($n = 3$ for remdesivir group and $n = 4$ for PBS and A2-TFN groups). Differences were compared by one-way ANOVA with post-hoc multiple comparison. $***p < 0.01$, compared with PBS group. c) Lung tissues of infected hamsters were harvested for plaque assay. Detection limit: 100 p.f.u. mL^{-1} . Two samples in A2-TFN group were below the detection limit. For statistical purpose, a value of 100 is assigned for these two samples. Representative images of d) H&E-stained lung tissue sections and e) immunofluorescence-stained lung tissue sections that harvested at 4 days post-infection from hamsters received different treatments. SARS-CoV-2 nucleocapsid protein (NP) was detected by specific antibody (green) and cell nuclei were stained by DAPI (blue). Scale bar 200 μm .

endpoint before 7 and 9 d.p.i., respectively (Figure 5b). The survival rate of A2-TFN group, zanamivir group, and unformulated tamibarotene group was significantly higher than that of PBS group ($p < 0.01$, Log-rank test). From 1 to 3 d.p.i., a decrease in body weight ($\approx 10\%$) was observed in mice treated with A2-TFN powder (Figure 5c), which is considered to be a side effect of powder insufflation to the lung of mice. Given the fact that this powder formulation was designed to have an aerodynamic size suitable for effective lung deposition in human, the side effect after i.t. administration in mice is expected due to the considerable anatomical difference between human and rodent. Starting from 4 d.p.i., the body weight of mice treated with

A2-TFN powder rose back to around 95% of baseline level, indicating the recovery of animals. In fact, we also monitored the body weight of uninfected mice following i.t. administration of SFD HPBCD and A2-TFN powder (Figure S3a, Supporting Information). A similar level of weight loss was observed after day 1 post-administration for both groups, although the HPBCD group recovered more rapidly than A2-TFN group. No marked toxicity was observed in the lung histopathology of the uninfected mice (Figure S3b, Supporting Information). On day 3 post-challenge, the viral RNA load in lung tissues harvested from mice treated with A2-TFN powder and unformulated tamibarotene were significantly lower than that of PBS-treated mice ($p < 0.01$, one-way

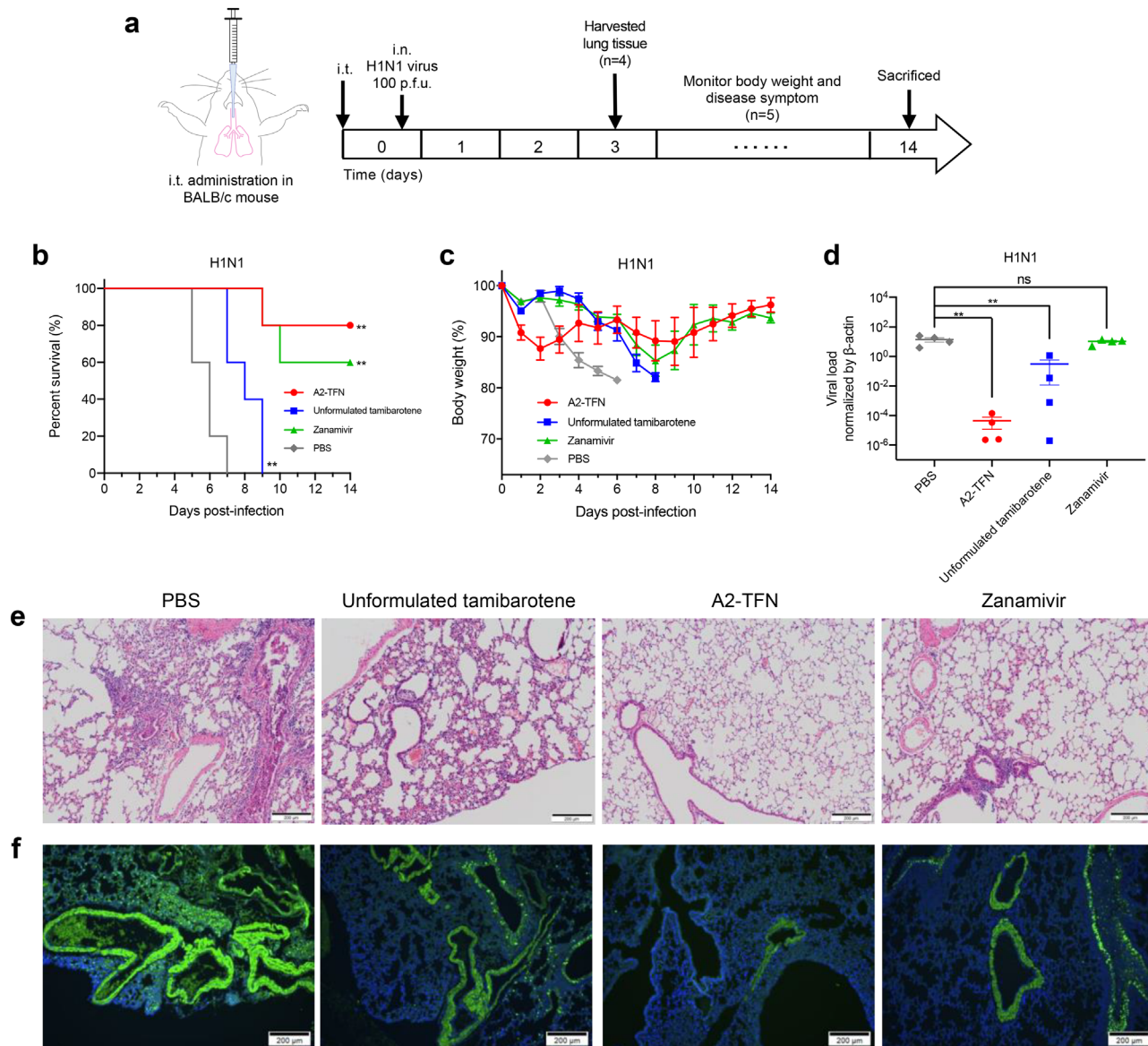


Figure 5. In vivo antiviral activity of tamibarotene formulation against H1N1 virus for prophylactic protection. a) Schematic of intratracheal (i.t.) administration in BALB/c mice and the schedule of experimental protocol. Each mouse received either PBS, unformulated tamibarotene suspension, A2-TFN powder, or zanamivir solution via i.t. administration prior to intranasal (i.n.) inoculation of H1N1 virus. b) Survivals were monitored for 14 days or until the human endpoint was reached ($n = 5$). The survival rates in each group were compared using Log-rank test (Mantel-Cox). ** $p < 0.01$, compared with PBS group. c) Daily body weights of surviving mice were presented as percentage of baseline level ($n = 5$); d) lung tissues were harvested at 3 days post-infection for viral load assay ($n = 4$). Differences were compared by one-way ANOVA with post-hoc multiple comparison. ** $p < 0.01$, ns: not significant, compared with PBS group. Representative images of e) H&E-stained lung tissue section and f) immunofluorescence-stained lung tissue sections from infected mice received different treatments. H1N1 PA protein was detected by specific antibody (green) and cell nuclei were stained by DAPI (blue). Scale bar 200 μ m.

ANOVA) (Figure 5d). There was no significant difference in viral load between PBS group and zanamivir group. Histopathological examination of hematoxylin and eosin (H&E)-stained lung tissues was conducted at 3 d.p.i. (Figure 5e). As expected, severe alveolar damage and interstitial inflammatory infiltration were observed in the lung tissue of mice treated with PBS and unformulated tamibarotene, albeit to a less extent for the latter. In contrast, the alveolar damage and interstitial infiltration were alleviated in the lung tissues of mice treated with A2-TFN powder

and zanamivir. Immunofluorescence staining demonstrated that massive viral PA protein expression was seen in the diffuse alveolar areas and in the focal bronchiolar epithelial cells from the mice treated with PBS (Figure 5f). In the lung tissues of mice treated with unformulated tamibarotene and zanamivir, viral PA protein expression in diffuse alveolar region was diminished but remained noticeable in bronchiolar epithelial cells. The expression of PA protein was largely suppressed in both alveolar and bronchiolar region in the lung tissue of A2-TFN-treated mice.

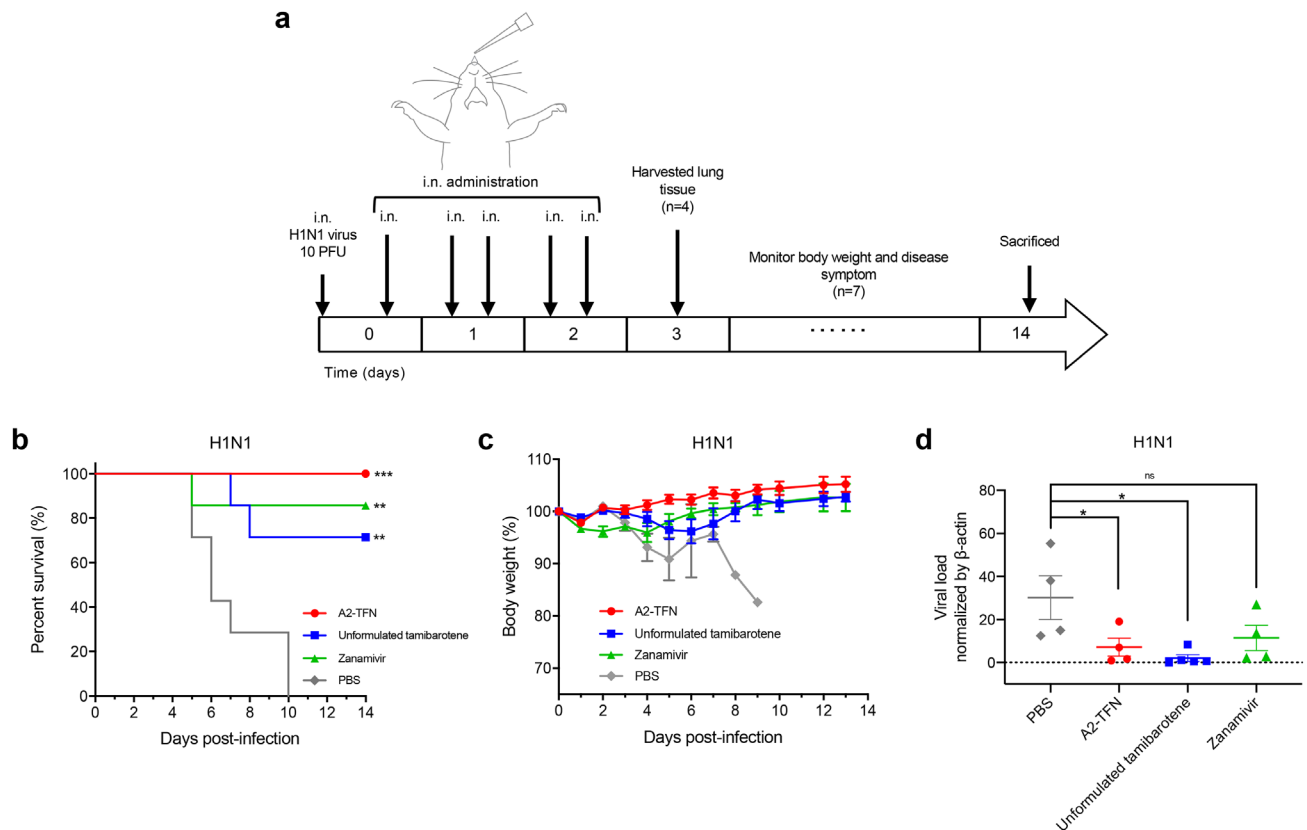


Figure 6. In vivo antiviral activity of tamibarotene formulation against H1N1 virus for therapeutic intranasal (i.n.) treatment. a) Schematic of i.n. administration in BALB/c mice and the schedule of experimental protocol. b) Survivals were monitored for 14 days or until the humane endpoint was reached ($n = 7$). The survival rates in each group were compared using Log-rank test (Mantel-Cox). *** $p < 0.001$, ** $p < 0.01$, compared with PBS group. c) Daily body weights of surviving mice were presented as percentage of baseline level ($n = 7$); d) lung tissues were harvested at 3 days post-infection for viral load assay ($n = 4$). Differences were compared by one-way ANOVA with post-hoc multiple comparison. * $p < 0.05$, ns: not significant, compared with PBS group.

Taken together, these results suggested that a single prophylactic dose of A2-TFN via i.t. administration could protect the mice from the highly pathogenic H1N1 virus challenge with an efficacy comparable to, if not better than, the commercially available anti-influenza drug zanamivir.

With the excellent protection provided by a single prophylactic dose of inhaled tamibarotene powder against H1N1 virus, we further investigated the therapeutic effect of tamibarotene powder reconstitution administered by i.n. administration (Figure 6). After i.n. inoculation with 10 p.f.u. of H1N1 virus, the mice received reconstituted A2-TFN solution, unformulated tamibarotene suspension, or zanamivir solution via i.n. administration. The dose of tamibarotene and zanamivir was 0.1 and 2 mg kg⁻¹, respectively. The fourth group of mice received 20 μ L of PBS solution by i.n. administration as negative control. A total of five therapeutic doses were delivered. At 14 d.p.i., the survival rate of A2-TFN reconstitution group was 100%, whereas survival rates of zanamivir group and unformulated tamibarotene group were 86% and 71%, respectively (Figure 6b). With all the mice in PBS group reaching humane endpoint by 10 d.p.i., the survival rate of mice in A2-TFN group, zanamivir group and unformulated tamibarotene group was significantly higher than that of PBS group ($p < 0.01$, Log-rank test). No remarkable body weight loss and disease symp-

tom were recorded from the mice treated with A2-TFN reconstitution throughout the 14-day monitoring (Figure 6c). On 3 d.p.i., the lung tissues of mice in each group were harvested for viral RNA load assay (Figure 6d). The viral load in A2-TFN reconstitution group and unformulated tamibarotene group were significantly lower than that of PBS group ($p < 0.05$, one-way ANOVA), while the viral load in zanamivir group and PBS group were not significantly different ($p > 0.05$, one-way ANOVA). The above results indicated that, in addition to single dose prophylaxis of tamibarotene powder delivered via i.t. route, i.n. administration of reconstituted tamibarotene powder solution and unformulated tamibarotene suspension can also practically protect the mice from H1N1 viral infection.

In summary, we have successfully demonstrated the broad-spectrum protective antiviral efficacy of A2-TFN powder formulation against SARS-CoV-2, MERS-CoV, and H1N1 virus following single prophylactic dose administered via the pulmonary route in vivo, as well as therapeutic effect against H1N1 via the intranasal route. The efficacy of SFD tamibarotene formulation and its reconstitution were superior to the unformulated tamibarotene and comparable to or even better than the commercially available antiviral agents remdesivir (against SARS-CoV-2) and zanamivir (against H1N1 virus).

3. Discussion

In the present work, we reported an inhalable powder formulation of tamibarotene with broad-spectrum antiviral activity, which can potentially serve as a therapy for prevention and treatment of respiratory viral infections. During the outbreak of emerging and re-emerging epidemics, especially the ones caused by unknown pathogens, the identification of pathogens and the development of specific antiviral or preventive vaccine could be very time-consuming.^[27] Therefore, applying a safe and potent broad-spectrum antiviral therapy at the early onset of infection is of utmost importance to control the epidemics and improve patient's outcome. Ideally, such a formulation should be safe and easy to administer for emergency use. Since the respiratory tract is typically the portal of entry of viruses that cause respiratory infections, with the lower respiratory tract is usually the primary site of infections, it is rational to deliver antivirals by inhalation to maximize drug concentration in the lung. Here, we hypothesized that repurposing and reformulating a commercially available retinoid derivative, tamibarotene, into inhalable powder for pulmonary delivery could improve lung distribution while minimizing systemic exposure, such that effective antiviral activity against different categories of viruses can be achieved without an extremely high dose.

Among different dosage forms for pulmonary delivery, inhaled dry powder is preferred because of its better stability, lower risk of microbial contamination and easier administration compared to the liquid counterpart.^[28] Moreover, inhalation of dry powder is non-invasive with the possibility of self-administration, making it particular suitable for use in out-patients during early control of infections and reduces the burden on the healthcare system.^[29] Given the fact that tamibarotene has a poor solubility, we intended to improve the solubility and enhance the dissolution rate of tamibarotene through formulation. Herein we demonstrated that A2-TFN powder formulation prepared by SFD exhibited excellent aerosol properties with a high respirable fraction in the cascade impactor study, and an accelerated dissolution rate in the dissolution study. The accelerated dissolution rate of SFD formulation was attributed to a combined effect of porous structure of the particle and the complexation between drug and HPBCD. When solvent sublimed in the freeze drying process, the frozen crystal transit from solid to gas phase, leaving pores in the resultant solid particle. The porous structure increases the surface area of particle to allow rapid dissolution. In other pulmonary drug delivery studies, polymers such as poly(L-lactic acid) and poly(lactic-co-glycolic acid), or lipids in forms of liposomes and solid lipid nanoparticles were commonly incorporated in inhaled dry powder formulations.^[30] These excipients are associated with problems such as safety concerns and stability issues.^[31] Here, HPBCD, which has a good safety profile for pulmonary delivery,^[31b,32] was employed as the sole excipient to function as solubilizer. With desirable properties for pulmonary delivery, the simple composition may allow the possibility of accelerated production. Moreover, in contrast to the poor lung distribution after systemic administration of tamibarotene, the rapid drug absorption and higher bioavailability following pulmonary delivery of A2-TFN powder in pharmacokinetic study elucidated the benefits of topical delivery to the airways for local antiviral action.

We further demonstrated the broad-spectrum antiviral effect of SFD tamibarotene powder against SARS-CoV-2, MERS-CoV, and H1N1 virus with a prophylactic single-dose administration via pulmonary route, as well as the therapeutic antiviral effect against H1N1 with lower doses delivered by i.n. administration. Unsurprisingly, A2-TFN formulation was more effective than the unformulated tamibarotene due to the improved solubility, hence better activity. In H1N1-infected animal model, both as prophylactic and therapeutic use, A2-TFN formulation and its reconstitution performed better (in terms of survival rate and viral load) than zanamivir which was approved for the treatment of influenza A. It is noted that the dose of tamibarotene (0.1 mg kg⁻¹) employed in the therapeutic study was much lower than that of zanamivir (2 mg kg⁻¹), in which a clinically relevant dose of zanamivir was used. Consistent with our previous results that demonstrated the *in vitro* antiviral efficacy of tamibarotene against MERS-CoV,^[10] a single dose of tamibarotene powder administered to the lung of mice could significantly reduce the viral yield of the lethal MERS-CoV in the lung tissue. Remarkably, the antiviral spectrum of tamibarotene also covers the SARS-CoV-2 that causes a global pandemic in 2020, as demonstrated in the hamster model with comparable efficacy to remdesivir after pulmonary administration. In contrast to inhaled tamibarotene, remdesivir is currently given through intravenous administration, which makes it difficult to provide on an outpatient basis. With the ease of administration, inhaled tamibarotene can be administered for prophylactic purpose or once mild symptom is developed, potentially widening the window of treatments. Moreover, remdesivir requires a complex synthesis process to manufacture, resulting in a high treatment cost and limited availability for only several million patients over the next few years. In view of the potentially-long epidemic dynamics and pressures on critical care capacity over the next few years, as well as the potential resurgence of SARS-CoV-2 in the future, inhalation of tamibarotene can be considered as one of the potential countermeasures for global control of the COVID-19 pandemic. Furthermore, it is worth mentioning that by the end of February 2021, no inhaled powder formulation is available on the market for the treatment of COVID-19. With the favorable safety profile of tamibarotene^[14] and based on our findings, phase 1 and 2 studies evaluating inhaled tamibarotene for its safety and as an at-home treatment for COVID-19 could be considered.

Targeting lipid reprogramming in host cell to interrupt virus life cycle equips tamibarotene with broad-spectrum antiviral activity and pan-coronavirus antiviral potential, which can make it advantageous in responding to mutated or drug-resistant virus strains. In addition, by demonstrating antiviral efficacy against SARS-CoV-2 and H1N1 virus in respective animal models, inhaled tamibarotene presents the potential as a solution for COVID-19 and influenza co-infection. Our recent work demonstrated that simultaneous or sequential co-infection by SARS-CoV-2 and influenza A(H1N1)pdm09 caused more severe disease than infection by either virus in hamsters.^[33] Prior influenza A(H1N1)pdm09 infection lowered SARS-CoV-2 pulmonary viral loads but enhanced lung damage. In this regard, inhaled tamibarotene can also be considered as an option for prophylaxis and therapy of SARS-CoV-2 and seasonal influenza A co-infection.

The overall outcomes of this work were encouraging, yet the formulation and regimen can be further optimized for better aerosol performance and antiviral therapy. As a proof-of-concept, we demonstrated a promising approach by preparing inhalable tamibarotene powder formulation using SFD technique with HPBCD as the sole excipient. While the aerosol performance of current formulation was satisfactory, the drug content can be further increased to allow flexible dosing for clinical application. In the anti-influenza experiments, apart from delivering the tamibarotene powder into the lower airways by pulmonary delivery, we also reconstituted SFD tamibarotene powder into solution for intranasal administration to examine the therapeutic effect of tamibarotene formulation after viral infection. The results demonstrated a potent efficacy of tamibarotene as liquid form against the pathogenic H1N1 virus by targeting the upper airways of mice. In fact, we have prepared inhalable tamibarotene powder by other drying methods (e.g., spray drying) and formulated tamibarotene as nasal powder to facilitate antiviral action in the upper airways (Table S1, Figure S1, Supporting Information). Further investigations are warranted to optimize the formulations for clinical use. It is evident that a single dose of SFD tamibarotene powder given by pulmonary delivery has successfully offered prophylactic broad-spectrum antiviral effect in animals, and the intranasal administration of reconstituted tamibarotene formulation also demonstrated therapeutic effect against influenza A virus. To extend the scope of therapeutic applications of inhaled tamibarotene powder, optimizing the dosage regimens of pulmonary delivered tamibarotene as a broad-spectrum antiviral therapy will be our next step of investigation. In regard to the rapid absorption of tamibarotene following pulmonary delivery, it is also within our interest to prolong the half-life of tamibarotene in the lung tissue by optimizing the formulation, thereby conferring elongated antiviral protection. We believe that this work provides valuable insight for the accelerated development of antiviral therapy by repurposing the existing drugs for the prevention and treatment of respiratory viral infections, and eventually contribute to epidemic and even pandemic control.

4. Experimental Section

Materials: Tamibarotene was purchased from Cayman Chemical (Michigan, USA). HPBCD was purchased from Sigma Aldrich (Saint Louis, USA). Tert-butyl alcohol (TBA) was obtained from Meryer Chemical Technology (Shanghai, China). Methanol and acetonitrile (HPLC grade) were purchased from Anaqua Chemicals Supply (Cleveland, USA). Acetic acid (HPLC grade) was obtained from Fisher Scientific (Loughborough, UK). All solvents and reagents were of analytical grade or better unless otherwise stated.

Spray Freeze Drying of Tamibarotene: The feed solution for SFD was first prepared by mixing the stock solutions of tamibarotene (10 mg mL⁻¹ in TBA) and HPBCD (100 mg mL⁻¹ in water) at 1:2 tamibarotene: HPBCD molar ratio to a final total solute concentration of 52.1 mg mL⁻¹. The solution was mixed and maintained at 37 °C (to prevent the freezing of TBA which had a freezing point of 25.4 °C) prior to spraying. A two-fluid nozzle (Büchi, stainless steel two-fluid nozzle with an internal diameter of 0.7 mm, Switzerland) operated at a gas flow rate of 601 L h⁻¹ was used for atomization. The feed solutions were loaded into a syringe which was connected to the nozzle and the liquid feed rate was controlled at 1.5 mL min⁻¹ by a syringe pump (LEGATO 210 Syringe Pump, KD Scientific, MA, USA). The atomized droplets were collected in a stainless-steel collector

containing liquid nitrogen to allow instant freezing. The frozen droplets were transferred into a freeze dryer (FreeZone 6 Liter Benchtop Freeze Dry System with Stoppering Tray Dryer, Labconco Corporation, Missouri, USA) which was programmed to maintain a primary drying temperature at -25 °C for 40 h, followed by a secondary drying in which the temperature was gradually increased to 20 °C in 4 h and the temperature was maintained for at least 20 h. The samples were kept a pressure below 0.14 mBar throughout the freeze-drying process. The dried products were collected and stored in desiccators with silica gel at ambient temperature until further analysis. The production yield was calculated as the percentage of the total mass of powder collected in the initial solute mass input.

Drug Quantification by High Performance Liquid Chromatography: Tamibarotene was quantified using high performance liquid chromatography (HPLC) with photodiode array detector (Agilent 1260 Infinity; Santa Clara, USA). A C-18 column (Agilent Prep-C18, 4.6 × 250 mm, 5 µm) was used with a mobile phase composed of acetonitrile and 5% acetic acid 80/20 v/v. A volume of 25 µL was injected and the running flow rate was set at 1 mL min⁻¹. Tamibarotene was detected at 280 nm with a retention time at 6.2 min. Tamibarotene was quantified against a standard curve in the range of 1.57 to 200 µg mL⁻¹. To determine the drug loading, SFD powder of tamibarotene were weighed and dissolved in methanol to a final volume of 5 mL. The sample was filtered through a 0.45-µm nylon membrane filter before quantified by HPLC as described above. The measurement of drug content in each formulation was performed in triplicate. Drug loading is defined as the ratio of tamibarotene detected in the formulation to the total amount of powder.

Scanning Electron Microscopy: The morphology of A2-TFN powder and the unformulated drug was visualized by field emission SEM (Hitachi S-4800 N, Tokyo, Japan) at 5 kV. The powders were sprinkled onto carbon stick tape which was mounted on SEM stubs, and excess powders were removed by clean air. The powders were sputter-coated using a sputter coater (Q150T PLUS Turbomolecular Pumped Coater, Quorum, UK) with ≈13 nm gold-palladium alloy in 90 s to avoid charging during SEM imaging.

Evaluation of Aerosol Performance by Cascade Impactors: The aerosol performance of A2-TFN powder for pulmonary delivery was evaluated using a NGI (Copley, Nottingham, UK) as previously described.^[19b] Briefly, ≈3 mg of A2-TFN powders were weighed and loaded into a size 3 capsules which were placed in a Breezhaler. The operating airflow rate was set at 90 L min⁻¹ with a pressure drop of 3.4 kPa. Prior to each dispersion, a thin layer of silicon grease (LPS Laboratories, Illinois, GA, USA) was coated onto the stages of NGI to reduce particle bounce. After dispersion of two capsules, methanol was used to rinse and dissolve the powder deposited on capsule, inhaler, adaptor, and each stage of NGI. The recovered dose was defined as the total mass of tamibarotene assayed by HPLC on all stages in a single run of impaction. The EF referred to the fraction of powder that exited the inhaler with respect to the recovered dose. FPD was the mass of particles with aerodynamic diameter less than 5.0 µm as calculated with the assayed tamibarotene obtained from HPLC in NGI experiment. FPF was defined as the percentage fraction of FPD with respect to the recovered dose.

Dissolution Study: The dissolution profile of A2-TFN powders was investigated using a jacketed beaker which contained 100 mL of simulated lung fluid as dissolution medium. The preparation of simulated lung fluid was according to Marques et al. (SLF3 in the article).^[34] The temperature was maintained at 37 °C and the medium was stirred at 75 rpm with a magnetic bar. As FPD (aerodynamic diameter < 5 µm) was considered to be the fraction of powder that could deposit in the deep lung region, the FPD of A2-TFN formulation was collected by a Fast Screening Impactor (FSI, Copley Scientific, UK) coupled with Breezhaler as described before^[19b] for dissolution study. ≈8.5 ± 0.5 mg of A2-TFN powder was dispersed by FSI to separate an FPD (which contained an estimated amount of 0.5 mg of tamibarotene). The powders were placed on a glass fiber filter paper which was then transferred into the jacketed beaker. At pre-determined time intervals, 1 mL of dissolution medium was withdrawn and filtered through 0.45 µm membrane filter. Equal volume of pre-warmed fresh medium was refilled immediately. The unformulated tamibarotene powder was included

as control for comparison. The concentration of tamibarotene was quantified by HPLC as described above. The dissolution study was carried out in triplicate.

Fourier-Transform Infrared Spectroscopy: FT-IR spectrum of A2-TFN powders and raw materials were obtained using Spectrum Two FT-IR spectrometer with UATR Accessory (PerkinElmer, USA). Appropriate amount of powder (less than 1 mg) was placed on the surface of the UATR crystal and pressed to form pellets. For each sample, the scanning range of spectra was 400–4000 cm^{-1} .

Differential Scanning Calorimetry: DSC (DSC 250, TA Instruments, Newcastle, DE, USA) was used to study the thermal response of raw materials and their physical mixture, as well as A2-TFN powders. ≈ 1 mg of powders were weighed and loaded into an aluminum crucible and heated from 50 to 280 $^{\circ}\text{C}$ at a constant rate of 10 $^{\circ}\text{C min}^{-1}$.

Animals and Ethics Approval: Healthy female BALB/c mice aged 7–9 weeks (body weight ≈ 20 g) were used to investigate the pharmacokinetic profile and anti-influenza effect of tamibarotene in animals following pulmonary delivery. hDPP4 transgenic C57BL/6 mice and golden Syrian hamster were used to investigate the antiviral effect against MERS-CoV and SARS-CoV-2 of tamibarotene following pulmonary delivery, respectively. The mice and hamsters were obtained from the Centre for Comparative Medicine Research of The University of Hong Kong (HKU) and were housed in a 12 h light/dark cycle with food and water available ad libitum. All the animal experiments were performed with the approval from the Committee on the Use of Live Animals in Teaching and Research (CULATR, approval number: CULATR 5587-20) at HKU and following the standard operating procedures of the Biosafety Level 2 and Level 3 animal facilities.^[35]

In Vivo Pharmacokinetic Study: The mice were randomly allocated to two treatment groups with 45 mice per group. The first group received 1 mg of A2-TFN powder formulation through i.t. administration under anesthesia as previously reported.^[36] The successful powder aerosolization after i.t. insufflation was evidenced by in vivo fluorescence imaging (Figure S4, Supporting Information). The second group received 200 μL of unformulated tamibarotene (0.5 mg mL^{-1} dissolved in 0.1% DMSO/PBS) by i.p. administration. Each mouse in both groups received 100 μg of tamibarotene. At specific time point post-administration, five mice in each group were euthanized by i.p. injection of pentobarbital (90 mg kg^{-1}). The blood sample was collected, and the lung tissues were harvested as previously described.^[37] Tamibarotene in plasma and lung homogenate was extracted by solid phase extraction cartridge (SOLA SAX, Thermo Scientific, USA) and the eluent was dried under a mild stream of nitrogen. The dry residue was reconstituted by HPLC mobile phase (5% acetic acid/acetonitrile 20/80), centrifuged, and the supernatant was assayed by HPLC. The concentration of tamibarotene was quantified against a standard curve ranged from 0.157 to 25 $\mu\text{g mL}^{-1}$ with blank plasma or lung homogenates as background. Pharmacokinetic parameters of both groups were analyzed using non-compartmental analysis (NCA) model with Phoenix WinNonLin 7.0 software.

In Vivo Antiviral Prophylactic Efficacy: Against SARS-CoV-2: Golden Syrian hamsters were used for studying in vivo prophylactic activity of A2-TFN formulation against SARS-CoV-2. The hamsters were divided into three groups (four hamsters per group). In the first two groups i.t. administration was performed under anesthesia: i) 200 μL of remdesivir solution (2.5 mg mL^{-1}); ii) 5 mg of A2-TFN powder. Remdesivir was prepared as 100 mg mL^{-1} stock in DMSO and further diluted using 12% sulfobutylether- β -cyclodextrin. The third group of hamsters received 200 μL of PBS via i.t. administration as negative control. The dose of remdesivir or tamibarotene was 5 mg kg^{-1} per hamster. Two hours after i.t. administration, hamsters were i.n. inoculated with 20 μL of virus suspension containing 10^5 p.f.u. of SARS-CoV-2 under anesthesia by i.p. injection of ketamine (200 mg kg^{-1}) and xylazine (10 mg kg^{-1}). All hamsters were euthanized on 4 d.p.i. and the lung tissues were collected for further analysis. Viral load in lung homogenates was measured by qRT-PCR method.^[38] The lung tissue histopathology of infected hamster was examined by H&E and immunofluorescence staining as previously described.^[25] This experiment was conducted in one independent experiment ($n = 4$ in each group).

In Vivo Antiviral Prophylactic Efficacy: Against MERS-CoV: hDPP4 transgenic C57BL/6 mice were used for investigating in vivo prophylactic activity of A2-TFN formulation against MERS-CoV. The mice were divided into three groups (five mice per group) for i.t. administration under anesthesia of: i) 20 μL of unformulated tamibarotene suspension (1 mg mL^{-1}); ii) 1 mg of A2-TFN powder; and iii) 20 μL of PBS (negative control). The dose of tamibarotene in the first two groups was 5 mg kg^{-1} per mouse. Two hours after i.t. administration, hDPP4 mice were i.n. inoculated with 20 μL of virus suspension containing 100 p.f.u. MERS-CoV under anesthesia. All mice were euthanized on 3 d.p.i. and the lung tissues were collected for further analysis. Viral load in lung tissue homogenates was measured by qRT-PCR method as previously described.^[10] This experiment was conducted in one independent experiment ($n = 5$ in each group).

In Vivo Antiviral Prophylactic Efficacy: Against H1N1 Virus: BALB/c mice were used to investigate the in vivo activity of A2-TFN formulation against influenza A H1N1 virus. The mice were divided into four groups (nine mice per group). Prior to virus inoculation, i.t. administration was performed under anesthesia in each group: i) 20 μL of zanamivir solution (5 mg mL^{-1}); ii) 50 μL of unformulated tamibarotene suspension (2 mg mL^{-1}); and iii) 1 mg of A2-TFN powder. The dose of zanamivir or tamibarotene was 5 mg kg^{-1} per mouse. In the fourth group of mice, 50 μL of PBS was i.t. administered as negative control. At 2 h post administration, all the mice were i.n. inoculated with 20 μL of virus suspension containing 100 p.f.u. of H1N1 virus under anesthesia. Four mice in each group were euthanized randomly on 3 d.p.i. and the lung tissues were harvested for viral load assay by qRT-PCR method. Animal survival, clinical symptoms, and body weight were monitored for 14 days or until the humane endpoint (body weight loss more than 20%) was reached. The lung tissue histopathology of infected mice was examined by H&E and immunofluorescence staining as previously described.^[39] This experiment was conducted in two independent experiments ($n = 9$ in each group).

In Vivo Antiviral Therapeutic Efficacy: Against H1N1 Virus: To evaluate the therapeutic effect of tamibarotene formulation against H1N1 virus, BALB/c mice were i.n. inoculated with 20 μL of virus suspension containing 10 p.f.u. of H1N1 virus under anesthesia. At 4 h post virus challenge, the first therapeutic dose was initiated and the mice were divided into four groups (11 mice per group) to receive 20 μL of each treatment via i.n. administration: i) zanamivir solution (2 mg mL^{-1}); ii) unformulated tamibarotene suspension (100 $\mu\text{g mL}^{-1}$); iii) reconstituted A2-TFN solution (100 $\mu\text{g mL}^{-1}$); and iv) PBS (as negative control). The dose of tamibarotene was 0.1 mg kg^{-1} , and the dose of zanamivir was 2 mg kg^{-1} . On day 1 and day 2 post-infection, the therapeutic doses were administered twice a day. On 3 d.p.i., four mice in each group were euthanized randomly and the lung tissues were harvested for viral load assay by qRT-PCR method. Animal survival, clinical symptoms and body weight were monitored for 14 days or until the humane endpoint (body weight loss more than 20%) was reached. This experiment was conducted in two independent experiments ($n = 11$ in each group).

Plaque Reduction Assay for Determination of Antiviral EC_{50} : Plaque reduction assay was performed to plot the 50% antiviral effective dose (EC_{50}) as previously described with slight modifications.^[40] Vero E6 cells were used for SARS-CoV-2 and MDCK cells for influenza A virus. Briefly, cells were seeded at 4×10^5 cells per well in 12-well tissue culture plates on the day before carrying out the assay. After 24 h of incubation, 50 p.f.u. of SARS-CoV-2 or H1N1 virus were added to the cell monolayer with or without the addition of drug compounds and the plates were further incubated for 1 h at 37 $^{\circ}\text{C}$ in 5% CO_2 before removal of unbound viral particles by aspiration of the media and washing once with DMEM. Monolayers were then overlaid with media containing 1% low melting agarose (Cambrex Corporation, New Jersey, USA) in DMEM and appropriate concentrations of individual compound, inverted and incubated as above for another 72 h. The wells were then fixed with 10% formaldehyde (BDH, Merck, Darmstadt, Germany) overnight. After removal of the agarose plugs, the monolayers were stained with 0.7% crystal violet (BDH, Merck) and the plaques counted. The percentage of plaque inhibition relative to the control (i.e., without the addition of compound) wells were determined for each drug compound concentration. The EC_{50} was calculated using Sigma

plot (SPSS) in an Excel add-in ED50V10. The plaque reduction assay experiments were performed in triplicate and repeated twice for confirmation.

Statistical Analysis: Statistical analyses were conducted using Graph-Pad Prism 8.0 for Student's *t*-test, ANOVA, and Log-rank (Mantel-Cox) test as indicated in the text or figure captions. The sample size (*n*) was indicated in the text or figure captions for each experiment. *p*-value < 0.05 was considered as statistically significant throughout this study.

Supporting Information

Supporting Information is available from the Wiley Online Library or from the author.

Acknowledgements

Q.L. and S.Y. contributed equally to this work. This work is financially supported by Seed Funding for Strategic Interdisciplinary Research Scheme, HKU; the Health and Medical Research Fund (grant no. 19180502 and CID-HKU1-11), Food and Health Bureau, The Government of the Hong Kong Special Administrative Region; General Research Fund (grant no. 17126919), the Research Grants Council (RGC) of Hong Kong; Innovation and Technology Fund (ITF); and donations from Lee Wan Keung Charity Foundation Limited, Marina Man-Wai Lee, the Hong Kong Hainan Commercial Association South China Microbiology Research Fund, and Lo Ying Shek Chi Wai Foundation. The authors would like to thank Mr. Godfrey Man and Mr. Ray Lee (Department of Pharmacology and Pharmacy, HKU) for their kind assistance in preparing the device for intratracheal administration in hamster.

Conflict of Interest

J.F.-W.C. has received travel grants from Pfizer Corporation Hong Kong and Astellas Pharma Hong Kong Corporation Limited, and was an invited speaker for Gilead Sciences Hong Kong Limited and Luminex Corporation. The other authors declared no conflict of interests. The funding sources had no role in study design, data collection, analysis or interpretation or writing of the report.

Data Availability Statement

Research data are not shared.

Keywords

broad-spectrum antiviral drugs, drug repurposing, influenza, pulmonary delivery, severe acute respiratory syndrome coronavirus 2

Received: March 3, 2021

Revised: April 17, 2021

Published online: June 10, 2021

- [1] V. C. Cheng, K. K. To, H. Tse, I. F. Hung, K. Y. Yuen, *Clin. Microbiol. Rev.* **2012**, *25*, 223.
 [2] V. C. Cheng, S. K. Lau, P. C. Woo, K. Y. Yuen, *Clin. Microbiol. Rev.* **2007**, *20*, 660.
 [3] J. F. Chan, S. K. Lau, K. K. To, V. C. Cheng, P. C. Woo, K. Y. Yuen, *Clin. Microbiol. Rev.* **2015**, *28*, 465.

- [4] a) J. F. Chan, S. Yuan, K. H. Kok, K. K. To, H. Chu, J. Yang, F. Xing, J. Liu, C. C. Yip, R. W. Poon, H. W. Tsoi, S. K. Lo, K. H. Chan, V. K. Poon, W. M. Chan, J. D. Ip, J. P. Cai, V. C. Cheng, H. Chen, C. K. Hui, K. Y. Yuen, *Lancet* **2020**, *395*, 514; b) J. S. Peiris, Y. Guan, K. Y. Yuen, *Nat. Med.* **2004**, *10*, S88; c) A. Zumla, D. S. Hui, S. Perlman, *Lancet* **2015**, *386*, 995.
 [5] a) J. Wang, Y. Peng, H. Xu, Z. Cui, R. O. Williams, 3rd, *AAPS Pharm-SciTech* **2020**, *21*, 225; b) J. Zhao, S. Zhao, J. Ou, J. Zhang, W. Lan, W. Guan, X. Wu, Y. Yan, W. Zhao, J. Wu, J. Chodosh, Q. Zhang, *Front. Immunol.* **2020**, *11*, 602256.
 [6] The RECOVERY Collaborative Group, *N. Engl. J. Med.* **2020**, *384*, 693.
 [7] D. M. Weinreich, S. Sivapalasingam, T. Norton, S. Ali, H. Gao, R. Bhore, B. J. Musser, Y. Soo, D. Rofail, J. Im, C. Perry, C. Pan, R. Hosain, A. Mahmood, J. D. Davis, K. C. Turner, A. T. Hooper, J. D. Hamilton, A. Baum, C. A. Kyratsous, Y. Kim, A. Cook, W. Kampman, A. Kohli, Y. Sachdeva, X. Graber, B. Kowal, T. DiCioccio, N. Stahl, L. Lipsich, N. Braunstein, G. Herman, G. D. Yancopoulos, *N. Engl. J. Med.* **2021**, *384*, 238.
 [8] WHO Solidarity Trial Consortium, H. Pan, R. Peto, A. M. Henao-Restrepo, M. P. Preziosi, V. Sathiyamoorthy, Q. Abdoool Karim, M. M. Alejandria, C. Hernández García, M. P. Kieny, R. Malekzadeh, S. Murthy, K. S. Reddy, M. Roses Periago, P. Abi Hanna, F. Ader, A. M. Al-Bader, A. Alhasawi, E. Allum, A. Alotaibi, C. A. Alvarez-Moreno, S. Appadoo, A. Asiri, P. Aukrust, A. Barratt-Due, S. Bellani, M. Branca, H. B. C. Cappel-Porter, N. Cerrato, T. S. Chow, N. Como, et al., *N. Engl. J. Med.* **2021**, *384*, 497.
 [9] a) N. Altan-Bonnet, *Trends Cell Biol.* **2017**, *27*, 201; b) J. Munger, B. D. Bennett, A. Parikh, X. J. Feng, J. McArdle, H. A. Rabitz, T. Shenk, J. D. Rabinowitz, *Nat. Biotechnol.* **2008**, *26*, 1179.
 [10] S. Yuan, H. Chu, J. F.-W. Chan, Z.-W. Ye, L. Wen, B. Yan, P.-M. Lai, K.-M. Tee, J. Huang, D. Chen, *Nat. Commun.* **2019**, *10*, 120.
 [11] a) N. S. Heaton, R. Perera, K. L. Berger, S. Khadka, D. J. LaCount, R. J. Kuhn, G. Randall, *Proc. Natl. Acad. Sci. USA* **2010**, *107*, 17345; b) K. A. Mayer, J. Stöckl, G. J. Zlabinger, G. A. Gualdoni, *Front. Immunol.* **2019**, *10*, 1533.
 [12] a) L. M. Kleinfelter, R. K. Jangra, L. T. Jae, A. S. Herbert, E. Mittler, K. M. Stiles, A. S. Wirchnianski, M. Kielian, T. R. Brummelkamp, J. M. Dye, K. Chandran, *mBio* **2015**, *6*, e00801; b) J. Petersen, M. J. Drake, E. A. Bruce, A. M. Riblett, C. A. Didigu, C. B. Wilen, N. Malani, F. Male, F. H. Lee, F. D. Bushman, S. Cherry, R. W. Doms, P. Bates, K. Briley, Jr., *PLoS Pathog.* **2014**, *10*, e1003911.
 [13] S. Yuan, C. C.-Y. Chan, K. K.-H. Chik, J. O.-L. Tsang, R. Liang, J. Cao, K. Tang, J.-P. Cai, Z.-W. Ye, F. Yin, *Viruses* **2020**, *12*, 628.
 [14] I. Miwako, H. Kagechika, *Drugs Today* **2007**, *43*, 563.
 [15] Q. T. Zhou, S. S. Leung, P. Tang, T. Parumasivam, Z. H. Loh, H. K. Chan, *Adv Drug Delivery Rev* **2015**, *85*, 83.
 [16] G. Reychler, L. Vecellio, J. C. Dubus, *Respir. Med. Res.* **2020**, *78*, 100778.
 [17] M. E. Davis, M. E. Brewster, *Nat. Rev. Drug Discovery* **2004**, *3*, 1023.
 [18] D. A. Vishali, J. Monisha, S. K. Sivakamasundari, J. A. Moses, C. Anandharamakrishnan, *J Control Release* **2019**, *300*, 93.
 [19] a) W. Liang, M. Y. Chow, S. F. Chow, H.-K. Chan, P. C. Kwok, J. K. Lam, *Int. J. Pharm.* **2018**, *552*, 67; b) Q. Liao, I. C. H. Lam, H. H. S. Lin, L. T. L. Wan, J. C. K. Lo, W. Tai, P. C. L. Kwok, J. K. W. Lam, *Int. J. Pharm.* **2020**, *584*, 119444; c) S. Wanning, R. Suverkrup, A. Lamprecht, *Int. J. Pharm.* **2015**, *488*, 136.
 [20] H.-K. Chan, *J. Aerosol Med.* **2006**, *19*, 21.
 [21] a) B. Chaurasiya, Y.-Y. Zhao, *Pharmaceutics* **2021**, *13*, 31; b) M. Hop-pentocht, P. Hagedoorn, H. W. Frijlink, A. H. de Boer, *Adv. Drug Deliv-ery Rev.* **2014**, *75*, 18.
 [22] a) M. L. Levy, W. Carroll, J. L. Izquierdo Alonso, C. Keller, F. Lavorini, L. Lehtimäki, *Adv. Ther.* **2019**, *36*, 2547; b) P. Rogliani, L. Calzetta, A. Coppola, F. Cavalli, J. Ora, E. Puxeddu, M. G. Matera, M. Cazzola, *Respir. Med.* **2017**, *124*, 6.

- [23] a) M. T. Esclusa-Diaz, M. Guimaraens-Méndez, M. B. Pérez-Marcos, J. L. Vila-Jato, J. J. Torres-Labandeira, *Int. J. Pharm.* **1996**, *143*, 203; b) E. Rodier, H. Lochard, M. Sauceau, J.-J. Letourneau, B. Freiss, J. Fages, *Eur. J. Pharm. Sci.* **2005**, *26*, 184.
- [24] A. Schittny, J. Huwyler, M. Puchkov, *Drug Delivery* **2020**, *27*, 110.
- [25] J. F. Chan, A. J. Zhang, S. Yuan, V. K. Poon, C. C. Chan, A. C. Lee, W. M. Chan, Z. Fan, H. W. Tsoi, L. Wen, R. Liang, J. Cao, Y. Chen, K. Tang, C. Luo, J. P. Cai, K. H. Kok, H. Chu, K. H. Chan, S. Sridhar, Z. Chen, H. Chen, K. K. To, K. Y. Yuen, *Clin. Infect. Dis.* **2020**, *71*, 2428.
- [26] S. Yuan, R. Wang, J. F. Chan, A. J. Zhang, T. Cheng, K. K. Chik, Z. W. Ye, S. Wang, A. C. Lee, L. Jin, H. Li, D. Y. Jin, K. Y. Yuen, H. Sun, *Nat. Microbiol.* **2020**, *5*, 1439.
- [27] a) M. Ghaebi, A. Osali, H. Valizadeh, L. Roshangar, M. Ahmadi, *J. Cell. Physiol.* **2020**, *235*, 9098; b) B. F. Haynes, L. Corey, P. Fernandes, P. B. Gilbert, P. J. Hotez, S. Rao, M. R. Santos, H. Schuitemaker, M. Watson, A. Arvin, *Sci. Transl. Med.* **2020**, *12*, eabe0948.
- [28] P. Colombo, F. Buttini, W. T. Wui, in *Inhalation Drug Delivery* (Eds: P. Colombo, D. Traini, F. Buttini), John Wiley & Sons, Hoboken **2013**, p.169.
- [29] A. H. de Boer, P. Hagedoorn, M. Hoppentocht, F. Buttini, F. Grasmeijer, H. W. Frijlink, *Expert Opin. Drug. Delivery* **2017**, *14*, 499.
- [30] a) F. Andrade, D. Rafael, M. Videira, D. Ferreira, A. Sosnik, B. Sarmiento, *Adv. Drug Delivery Rev.* **2013**, *65*, 1816; b) S. Chennakesavulu, A. Mishra, A. Sudheer, C. Sowmya, C. Suryaprakash Reddy, E. Bhargava, *Asian J Pharm. Sci.* **2018**, *13*, 91; c) M. C. Gaspar, A. Pais, J. J. S. Sousa, J. Brillaut, J. C. Olivier, *Int. J. Pharm.* **2019**, *556*, 117; d) E. Nemati, A. Mokhtarzadeh, V. Panahi-Azar, A. Mohammadi, H. Hamishehkar, M. Mesgari-Abbasi, J. Ezzati Nazhad Dolatabadi, M. de la Guardia, *AAPS PharmSciTech* **2019**, *20*, 120; e) T. Parumasivam, S. S. Leung, D. H. Quan, J. A. Triccas, W. J. Britton, H. K. Chan, *Eur. J. Pharm. Sci.* **2016**, *88*, 1; f) C. Thomas, A. Rawat, L. Hope-Weeks, F. Ahsan, *Mol. Pharm.* **2011**, *8*, 405.
- [31] a) M. Beck-Broichsitter, O. M. Merkel, T. Kissel, *J Control. Release* **2012**, *161*, 214; b) G. Pilcer, K. Amighi, *Int. J. Pharm.* **2010**, *392*, 1.
- [32] a) G. Dufour, W. Bigazzi, N. Wong, F. Boschini, P. de Tullio, G. Piel, D. Cataldo, B. Evrard, *Int. J. Pharm.* **2015**, *495*, 869; b) B. Evrard, P. Bertholet, M. Gueders, M. P. Flament, G. Piel, L. Delattre, A. Gayot, P. Leterme, J. M. Foidart, D. Cataldo, *J Control. Release* **2004**, *96*, 403; c) M. Guan, R. Shi, Y. Zheng, X. Zeng, W. Fan, Y. Wang, W. Su, *Molecules* **2020**, *25*, 554; d) T. Loftsson, P. Jarho, M. Måsson, T. Järvinen, *Expert Opin. Drug. Delivery* **2005**, *2*, 335; e) L. Matilainen, T. Toropainen, H. Vihola, J. Hirvonen, T. Järvinen, P. Jarho, K. Järvinen, *J. Control. Release* **2008**, *126*, 10.
- [33] A. J. Zhang, A. C.-Y. Lee, J. F.-W. Chan, F. Liu, C. Li, Y. Chen, H. Chu, S.-Y. Lau, P. Wang, C. C.-S. Chan, V. K.-M. Poon, S. Yuan, K. K.-W. To, H. Chen, K.-Y. Yuen, *Clin. Infect. Dis.* **2020**.
- [34] M. R. Marques, R. Loebenberg, M. Almukainzi, *Dissolution Technol* **2011**, *18*, 15.
- [35] a) S. Yuan, H. Chu, J. Huang, X. Zhao, Z. W. Ye, P. M. Lai, L. Wen, J. P. Cai, Y. Mo, J. Cao, R. Liang, V. K. Poon, K. H. Sze, J. Zhou, K. K. To, Z. Chen, H. Chen, D. Y. Jin, J. F. Chan, K. Y. Yuen, *Sci. Adv.* **2020**, *6*, eaba7910; b) J. F. Chan, S. Yuan, A. J. Zhang, V. K. Poon, C. C. Chan, A. C. Lee, Z. Fan, C. Li, R. Liang, J. Cao, K. Tang, C. Luo, V. C. Cheng, J. P. Cai, H. Chu, K. H. Chan, K. K. To, S. Sridhar, K. Y. Yuen, *Clin. Infect. Dis.* **2020**, *71*, 2139.
- [36] Y. Qiu, Q. Liao, M. Y. Chow, J. K. Lam, *J. Vis. Exp.* **2020**, *161*, e61469.
- [37] Q. Liao, L. Yip, M. Y. Chow, S. F. Chow, H.-K. Chan, P. C. Kwok, J. K. Lam, *Int. J. Pharm.* **2019**, *560*, 144.
- [38] S. Yuan, J. F. W. Chan, K. K. H. Chik, C. C. Y. Chan, J. O. L. Tsang, R. Liang, J. Cao, K. Tang, L. L. Chen, K. Wen, J. P. Cai, Z. W. Ye, G. Lu, H. Chu, D. Y. Jin, K. Y. Yuen, *Pharmacol. Res.* **2020**, *159*, 104960.
- [39] S. Yuan, H. Chu, K. Zhang, J. Ye, K. Singh, R. Y. Kao, B. K. Chow, J. Zhou, B. J. Zheng, *J. Antimicrob. Chemother.* **2016**, *71*, 2489.
- [40] a) S. Yuan, H. Chu, J. Ye, K. Singh, Z. Ye, H. Zhao, R. Y. Kao, B. K. Chow, J. Zhou, B. J. Zheng, *Antiviral Res.* **2017**, *137*, 58; b) L. Riva, S. Yuan, X. Yin, L. Martin-Sancho, N. Matsunaga, L. Pache, S. Burgstaller-Muehlbacher, P. D. De Jesus, P. Teriete, M. V. Hull, M. W. Chang, J. F. Chan, J. Cao, V. K. Poon, K. M. Herbert, K. Cheng, T. H. Nguyen, A. Rubanov, Y. Pu, C. Nguyen, A. Choi, R. Rathnasinghe, M. Schotsaert, L. Miorin, M. Dejosez, T. P. Zwaka, K. Y. Sit, L. Martinez-Sobrido, W. C. Liu, K. M. White, et al., *Nature* **2020**, *586*, 113.